[11]T. Mitsui and C. T. Tomizuka, Phys. Rev. 137, A564 (1965).
[12]R. Mitsudo, K. Motizuki, and T. Nagamiya, J. Phys. Soc. Japan 20, 710 (1965).
[13]P. A. Fedders and P. C. Martin, Phys. Rev. 143, 245 (1965).
[14]J. G. Collins and G. K. White, in Progress in Low Temperature Physics, edited by C. J. Gorter (North-Holland Publishing Company, Amsterdam, The Netherlands, 1964), Vol. IV.
[15]F. Heiniger, E. Bucher, and J. Müller, Phys. Letters 19, 163 (1965).
[16]E. Bucher and K. Andres, to be published.
[17]L. F. Mattheiss, Phys. Rev. 139, A1893 (1965); T. L. Loucks, Phys. Rev. 139, A1181 (1965).
[18]B. I. Halperin and T. M. Rice (unpublished).
[19]The calculation of the conductivity is similar to that given by D. Jerome, T. M. Rice, and W. Kohn, Phys. Rev. 158, 962 (1967).
[20]S. A. Werner, A. Arrott, and H. Kendrich, Phys. Rev. 155, 528 (1967).
[21]Neutron experiments by H. B. Möller et al. [Solid State Commun. 2, 109 (1964)] also show a critical scattering which extends to temperatures well above T_N but which drops off rapidly for $T < T_N$.
[22]A. L. Trego and A. R. Mackintosh (to be published).

POLARIZATION AND INTENSITY OF RAMAN SCATTERING FROM PLASMONS AND PHONONS IN GALLIUM ARSENIDE

A. Mooradian and A. L. McWhorter
Lincoln Laboratory,* Massachusetts Institute of Technology, Lexington, Massachusetts
(Received 7 July 1967)

Raman scattering from plasmons and phonons in GaAs has recently been reported[1] in which the coupling between the longitudinal optic phonon modes and the longitudinal plasma modes was demonstrated. We report here the investigation of the polarization properties and relative intensities of the Raman-scattered light from these mixed plasmon-phonon modes in oriented single crystals of n-type GaAs. The results are in good agreement with theoretical predictions[2] and yield values for the Raman tensor and electro-optic coefficient of GaAs.

A neodymium-doped yttrium aluminum garnet laser with a cw output of 3 W at 1.06 μ was used to excite the collective excitations. The experimental arrangement has been described previously.[1] The samples were rectangular parallelepipeds $3 \times 3 \times 7$ mm in size with {100} faces, and were mounted on a cold finger in contact with liquid helium. The laser beam, after passing through a polarizer, was incident along a ⟨100⟩ axis of the crystal while the scattered light was collected at 90° along another ⟨100⟩ axis. The solid angle of collection was about 0.08 sr. The system response was determined as a function of polarization and wavelength by using a calibrated quartz-iodine light source.

Figure 1 is a plot of the Raman frequency shifts as a function of the square root of the electron concentration and shows the mixing between the longitudinal optic phonon mode of frequency ω_l and the longitudinal plasma mode of frequency $\omega_p = (4\pi e^2/\epsilon_\infty m^*)^{1/2}$. Here n is the electron concentration, m^* the conduction-band effective mass, and ϵ_∞ the optical dielectric constant. The Raman line shapes and polarization properties for a sample with $n = 1.9 \times 10^{18}$ cm^{-3} are shown in Fig. 2. The transverse optic (TO) mode at frequency ω_t is unaffected by the presence of the free car-

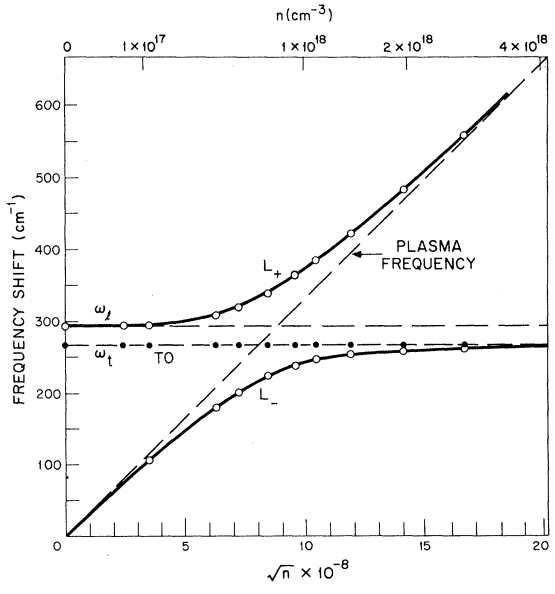

FIG. 1. Frequency shift of the Raman-scattered light in GaAs at room temperature as a function of the square root of the electron concentration. The solid curves labeled L_+ and L_- give the frequencies of the mixed longitudinal-phonon–plasmon modes calculated from the roots of the dielectric constant of Eq. (4); the dashed line labeled TO is the transverse optic mode at frequency ω_t.

riers and exhibits the polarization properties predicted by group theory for a zinc-blende insulator.[3] However, the polarization properties of the upper and lower longitudinal branches, L_+, and L_-, differ markedly from those found for a pure longitudinal optic (LO) mode in semi-insulating GaAs. The latter, in accordance with group-theory predictions, shows zero LO scattering in the present geometry when the incident and scattered beams are both polarized parallel to the plane of scattering ($\parallel,\parallel$) or both perpendicular to the plane of scattering ($\perp,\perp$). But in Fig. 2 it is apparent that the largest longitudinal mode scattering occurs for the ($\perp,\perp$) configuration.[4]

The strong ($\perp,\perp$) scattering is just what is predicted by recent theoretical calculations[2] which take into account the effects of charge-density fluctuations. For the experimental geometry and conditions these calculations give for the differential scattering cross sections of the longitudinal modes

$$\frac{d^2\sigma_l(\perp,\parallel)}{d\Omega d\omega}=\frac{d^2\sigma_l(\parallel,\perp)}{d\Omega d\omega}=\frac{\hbar V(n_\omega+1)}{2\pi^2c^4}\left|\frac{e^2\epsilon_\infty}{\hbar^2\omega_t m_0^2 a}\left(\frac{\pi/M}{\epsilon_0-\epsilon_\infty}\right)^{1/2}\left(1-\frac{\omega_p^2}{\omega^2}\right)R_{xy}^z-\tfrac{1}{2}\omega_i^2\epsilon_\infty^2 z_{41}\right|^2\mathrm{Im}\frac{1}{\epsilon_l(\omega)},\tag{1}$$

$$\frac{d^2\sigma_l(\perp,\perp)}{d\Omega d\omega}=\left(\frac{e^2}{m^*c^2}\right)^2\frac{\hbar q^2\epsilon_\infty^2\omega_p^4 V(n_\omega+1)}{4\pi^2e^2\omega^4}\left(\frac{E_G^2}{E_G^2-\hbar^2\omega_i^2}\right)^2\mathrm{Im}\frac{1}{\epsilon_l(\omega)},\tag{2}$$

$$\frac{d^2\sigma_l(\parallel,\parallel)}{d\Omega d\omega}=0,\tag{3}$$

where the scattering peaks occur for values of ω near the two zeros of the total longitudinal dielectric constant

$$\epsilon_l(\omega)=\epsilon_\infty\left[1-\frac{\omega_p^2}{\omega(\omega-i/\tau)}\right]+\frac{(\epsilon_0-\epsilon_\infty)\omega_t^2}{\omega_t^2-\omega^2}.\tag{4}$$

In the above equations R_{xy}^z is the Raman tensor arising from deformation potential coupling and z_{41} is the electro-optic coefficient (both as defined by Loudon[3]), q is the wave vector of the longitudinal modes, V the active volume of the crystal, n_ω the Bose-Einstein factor, m_0 the free electron mass, M the reduced mass density of the sublattices, a the lattice constant, ϵ_0 the static dielectric constant, E_G the optical energy gap, and ω_i the laser frequency. A phenomenological electron collision time τ has been included in (4); the phonon damping is omitted since it is negligible in comparison. When $\omega_p=0$, Eq. (1) reduces to that given by Loudon,[3] and in the limit of large E_G and zero lattice polarizability, Eq. (2) reduces to the usual expression[5] for free electron scattering. Burstein, Pinczuk, and Iwasa[6] have obtained results equivalent to (1) by using a phenomenological appraoch, but neglected the scattering by the electrons given in (2).

For the TO modes the integrated scattering cross section is[3]

$$\frac{d\sigma_t(\parallel,\parallel)}{d\Omega}=\frac{\hbar V(n_t+1)}{2\omega_t c^4}\left|\frac{e^2}{\hbar^2 m_0^2 a M^{1/2}}R_{xy}^z\right|^2,\tag{5}$$

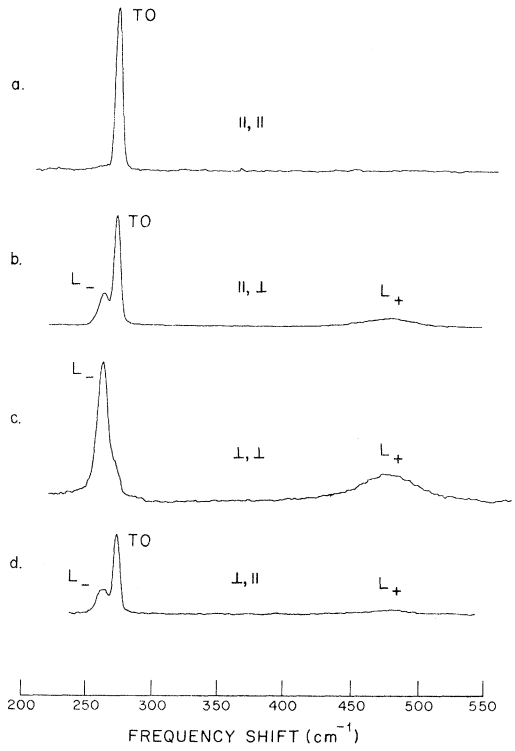

FIG. 2. Intensity and polarization properties of the Raman-scattered light from GaAs at liquid-helium temperature for a sample with $n=1.9\times10^{18}$ cm^{-3}. The scattering angle is 90° with the incident and scattered light along ⟨100⟩ directions. The pair of || and ⊥ signs by each trace gives the polarization of the incident and scattered light (in that order) with respect to the plane of scattering. The TO mode at 273 cm^{-1} has a true width of only about 1.5 cm^{-1}; in these traces it is considerably instrument broadened. The traces as shown are uncorrected for system response and the gain in trace (b) is lower than in the others.

with $\frac{1}{2}$ this amount for the $(\perp, \parallel)$ and $(\parallel, \perp)$ scattering, and zero for the $(\perp, \perp)$ scattering.

Within experimental error the Raman scattering from the two longitudinal modes could be fitted by line shapes consistent with (1)-(4). The electron collision time τ was found to be about 10^{-13} sec for the samples studied.

From the above equations it is seen that the relative integrated scattering intensities for all three modes involve only the unknowns $R_{xy}{}^{z}$ and z_{41}. The best fit between theory and experiment was obtained with $R_{xy}{}^{z} = 5 \times 10^{-59}$ cm g^3/sec^2 and $z_{41} = -1.0 \times 10^{-7}$ esu. Table I shows the measured and calculated results for two samples of relatively high electron concentration. The $(\parallel, \parallel)$ TO scattering has been normalized to unity.[7] In view of the experimental uncertainty (about $\pm 10\%$ for the TO and L_- modes, ± 15-20% for the L_+ mode) the agreement is quite satisfactory, except for the $(\perp, \perp)$ scattering of the L_+ mode for the $n = 1.9 \times 10^{18}$-cm^{-3} sample. The reason for this discrepancy is not understood.

The existence of a strong $(\perp, \perp)$ charge-density scattering for the L_- mode may seem puzzling until it is realized that in these samples we are dealing with a LO mode heavily screened by the conduction-band electrons. It is the screening charges that do the scattering. From the value obtained for $R_{xy}{}^{z}$ the deformation potential coupling should slightly dominate for the L_- mode when $n > 3 \times 10^{18}$ cm^{-3}, but for the samples of Table I the electro-optic coupling is not completely screened out and reduces the $(\parallel, \perp)$ and $(\perp, \parallel)$ scattering. It is predicted from (1) and has been confirmed experimentally that around $n = 4 \times 10^{17}$ cm^{-3} the electro-optic coupling just cancels the deformation potential coupling for the L_- mode, giving zero scattering for the $(\parallel, \perp)$ and $(\perp, \parallel)$ configurations.

Table I. Comparison of measured and calculated values of the integrated Raman scattering intensities for two samples of GaAs. The intensities are normalized to unity for the $(\parallel, \parallel)$ scattering of the TO mode.

Mode	Polarization	Scattering intensity $n = 1.4 \times 10^{18}$ cm^{-3} Meas.	Calc.	$n = 1.9 \times 10^{18}$ cm^{-3} Meas.	Calc.
TO	$\parallel, \parallel$	1.0	1.0	1.0	1.0
	$\perp, \perp$	0.06	0	0.03	0
	$\parallel, \perp$	0.47	0.5	0.51	0.5
	$\perp, \parallel$	0.50	0.5	0.49	0.5
L_-	$\parallel, \parallel$	0	0	0	0
	$\perp, \perp$	0.63	0.58	0.53	0.46
	$\parallel, \perp$	0.22	0.23	0.28	0.32
	$\perp, \parallel$	0.22	0.23	0.27	0.32
L_+	$\parallel, \parallel$	0	0	0	0
	$\perp, \perp$	1.3	1.4	1.3	1.9
	$\parallel, \perp$	0.9	0.95	0.8	0.94
	$\perp, \parallel$	0.9	0.95	0.7	0.94

It should be noted that according to theory[3] the values of $R_{xy}{}^{z}$ and z_{41} depend on ω_i. The present value for z_{41} corresponds to $\partial \chi_{yz}/\partial E_x = -\epsilon_\infty{}^2 z_{41}/4\pi \approx 1.0 \times 10^{-6}$ esu, a factor of 2 less than that deduced[6] from second-harmonic experiments, but almost exactly equal to the value determined by direct optical measurement on semi-insulating GaAs.[8] We have not attempted to obtain a deformation potential from $R_{xy}{}^{z}$ since it is not clear whether a two-band model will suffice. Additional experiments with $\hbar\omega_i$ more nearly equal to E_G should allow one to determine the difference between the conduction and valence band optical mode deformation potentials.

We thank G. B. Wright and P. N. Argyres for helpful discussions and D. J. Wells for assistance with the measurements.

*Operated with support from the U. S. Air Force.

[1]A. Mooradian and G. B. Wright, Phys. Rev. Letters 16, 999 (1966).

[2]A. L. McWhorter and P. N. Argyres, Bull. Am. Phys. Soc. 12, 102 (1967), and to be published.

[3]R. Loudon, Advan. Phys. 13, 423 (1964).

[4]The dominance of the $(\perp, \perp)$ scattering in Fig. 2 is actually somewhat exaggerated by the system response.

[5]See, for example, D. Pines, Elementary Excitations in Solids (W. A. Benjamin, Inc., New York, 1964), p. 206. The resonance enhancement factor $[E_G{}^2/(E_G{}^2 - \hbar^2\omega_i{}^2)^2]$ in (2) is the same factor found by P. A. Wolff, Phys. Rev. Letters 16, 225 (1966), for single-particle excitations and can result in a much greater scattering cross section than that calculated within the effective mass approximation [P. M. Platzman, Phys. Rev. 139, A379 (1965); A. L. McWhorter, in Physics of Quantum Electronics, edited by P. L. Kelley, B. Lax, and P. E. Tannenwald (McGraw-Hill Book Company, Inc., New York, 1966), p. 111]. It is assumed in (2) that only the virtual photon transitions that involve the direct energy gap are important.

[6]E. Burstein, A. Pinczuk, and S. Iwasa, Phys. Rev. 157, 611 (1967).

[7]The fit shown in Table I does not depend on the values chosen for such quantities as ϵ_∞, ϵ_0, m^*, or E_G since the relative scattering intensities really involve only two frequency ratios, ω_p/ω_t and ω_l/ω_t, which are determined from the Raman data, plus two adjustable normalized parameters, one proportional to

R_{xy}^{z} and the other to z_{41}/R_{xy}^{z}. However, the values subsequently deduced for R_{xy}^{z} and z_{41} do depend on other parameters. We took $\omega_t = 273$ cm^{-1}, $\omega_l = 296$ cm^{-1}, $\epsilon_\infty = 11.1$, $\epsilon_0 = (\omega_l/\omega_t)^2\epsilon_\infty = 13.1$, $m^* = 0.07m_0$, and $E_G = 1.50$ eV plus the electron Fermi energy and corresponding hole energy. The correct E_G to be used is somewhat ambigous because of the fairly high doping level involved, but fortunately the results are not too sensitive at liquid-helium temperature since there the resonance enhancement factor $[E_G^2/(E_G^2 - \hbar^2\omega_i^2)^2]$ is only about 4.

[8]V. S. Bagaev, Yu. N. Berozashvili, and L. V. Keldysh, Zh. Eksperim. i Teor. Fiz.–Pis'ma Redakt. 4, 364 (1966) [translation: JETP Letters 4, 246 (1966)].

MAGNETOINTERNAL FIELD EMISSION IN JUNCTIONS OF MAGNETIC INSULATORS*

L. Esaki, P. J. Stiles, and S. von Molnar
IBM Watson Research Center, Yorktown Heights, New York
(Received 24 March 1967; revised manuscript received 21 August 1967)

The observation of internal field emission (Fowler-Nordheim tunneling) in magnetically ordered insulators is reported. A large magnetic field effect was observed and interpreted as a decrease in the barrier height due to spin ordering.

We have observed an entirely new type of magnetointernal field emission effect in magnetically ordered insulators. This is the first time that a large magnetic field effect in internal field emission (or Fowler-Nordheim tunneling) has been reported. We employed here Eu chalcogenides such as EuSe and EuS, of which the magnetic transition temperatures have been reported to be 4.7 [1] and 16.5°K,[2] respectively. The transition temperature for EuS simply means the Curie temperature, whereas EuSe below the transition temperature has a complex field-dependent magnetic structure, being antiferromagnetic in zero field and ferromagnetic for moderate applied fields.

Experimental junctions were constructed simply by successive evaporations, metal, the Eu chalcogenide, and metal, on a heated sapphire substrate without breaking vacuum. Thus the thin film sandwiched between metal electrodes provides a barrier for electrons. We prepared more than 100 units, in which the thickness of the Eu chalcogenides ranges from 200 to 600 Å. Al and Au were used as the electrode metal. X-ray measurements showed the films to be polycrystalline with the same lattice constant as the bulk. The junction area is approximately 4×10^{-4} cm^2.

The current-voltage characteristics on a semilog plot for a 300-Å EuSe junction at 4.2°K are shown in the lower right-hand side of Fig. 1. It is seen that the curve markedly shifts to lower voltages with a magnetic field of 20 kOe. The curves are always symmetric with respect to the applied voltage. We have found that for all units made, current-voltage curves at high voltages approach an asymptote expressed by

$$I = (aV^2/d^2)\exp(-bd/V), \quad (1)$$

as shown in the upper left-hand side of Fig. 1, where a and b are constants of the material and d is the thickness. We have further verified that the application of magnetic fields affects only the constant b, making it small with increase in field.

We have made measurements of the temperature dependence of the current-voltage curves. The voltage at a given current level (normalized to its value at 4.2°K) was plotted as a function of temperature. The results are shown

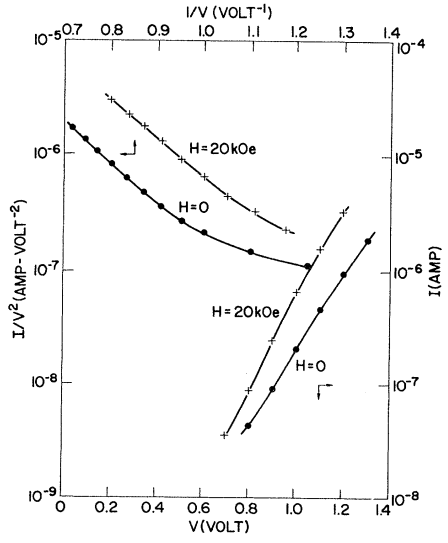

FIG. 1. Log$I$ vs V for EuSe at $H=0$ and 20 kOe in the lower right-hand side, log(I/V^2) vs I/V for EuSe at $H=0$ and 20 kOe in the upper left-hand side, at $T=4.2$°K.